7184 *Macromolecules* **2009**, *42*, 7184–7193
DOI: 10.1021/ma900787g

Macromolecules
ARTICLE

Structure of Aggregating Rod Suspensions Under Combined Shear and Electric Fields

Victor Pryamitsyn and Venkat Ganesan*

Department of Chemical Engineering, University of Texas at Austin, Austin, Texas 78712.

Received April 10, 2009; Revised Manuscript Received July 13, 2009

ABSTRACT: Efficient strategies for dispersion of carbon nanotubes in polymeric and solvent matrices constitutes an area of active interest. In this article, we examine from a theoretical perspective the hypothesis that a combination of AC electric and shear fields oriented at an angle may be used to enhance the dispersion of aggregated rod solutions. We present a deterministic and a Smoluchowski equation based analysis of the dynamics of homogeneous rod suspensions in a configuration involving combined electric and shear fields. We use this analysis to suggest that a cross-field shear and electric field configuration may potentially disperse aggregated nanotube suspensions. We test the predictions of our analytical models through Brownian dynamics simulations to analyze the dynamics of rod suspensions in a cross-field configuration. The results of our simulations display good agreement with our analytical results and serve to delineate the parametric regimes in which the use of a combination of electric and shear fields may enhance the dispersion of aggregated nanotubes.

Introduction

Recently, there has been a surge of interest in applications using polymer nanocomposite materials containing nanotubes dispersed in polymer matrices.[1−4] However, due to the propensity of nanotubes to aggregate into larger scale structures, many of the proposed applications are yet to reach their full potential.[2,5−7] Indeed, single-wall carbon nanotubes (SWNT) are characterized by strong van der Waals interactions with energies in the range of approximately 500 eV/μm of nanotube length. In conjunction with the large aspect ratio of nanotubes, such attractions lead to strong aggregation tendencies whereby the nanotubes typically form randomly oriented frozen bundles of the individual moieties.

A simple understanding of the causes of nanotube aggregation phenomena and the strategies explored for dispersion can be obtained by considering the second virial coefficient ν_2 for rodlike fluids. In general, the latter provides a quantitative measure of the tendency of a fluid of particles to phase separate (i.e. aggregate and precipitate). For a dilute suspension of hard rods ν_2 was calculated by Onsager, and can be written for weakly anisotropic suspensions) as[8−10]

$$\nu_2 = 2L^2d[1 - (0.035 + \varepsilon_{att})S_2{}^2 - O(\varepsilon_{att}d/L)] \qquad (1)$$

In the above, ε_{att} denotes the strength of attraction between the rods, and $S_2 \equiv \langle P_2(\cos\theta)\rangle$ with P_2 denoting the Legendre polynomial and θ the angle between the rod and the axis of alignment, represents the orientational order parameter of the rod suspension. One can see that if ε_{att} is positive and large, ν_2 may become negative and lead to aggregation of the rods. Moreover, it is evident that orientational ordering of the rod suspension ($S_2 > 0$), a state very likely at aspect ratios representative of nanotubes, substantially enhances the effect of attractions and renders the suspension more prone to aggregation.

*Corresponding author. E-mail: venkat@che.utexas.edu.

It is apparent from eq 1 that an obvious strategy to promote dispersion of nanotubes is to lower ε_{att}. Indeed, this idea forms the basis for numerous efforts which have explored functionalizing the nanotubes with oligomeric or polymeric compatibilizers to promote dispersion of the nanotubes.[2,3,6,11−13] In such situations, the compatibilizers contribute a repulsive force between the rods and reduce the attractive interactions.

Alternatively, it is also evident that nonequilibrium fields may be used to modulate S_2 (the state of orientational ordering in the system) and may provide a means to disperse aggregating nanotubes. *In this article, we explore whether the combined effects of shear and AC electric (or magnetic) fields can be used as a nonequilibrium means to influence the orientational order and thereby enhance the dispersion of aggregating nanotube suspensions*. Specifically, we present a hypothesis that while simple shear and electric fields alone may induce only an alignment of the rods, a setup involving shear and electric fields oriented at an angle to each other may lead to a state that promotes the dispersion of the rods. Experimentally, one may envision achieving such a setup in microfluidic channels where crossfield configurations of shear and electric fields may be realized.[14] In this article, we explore this hypothesis using a combination of analytical models and Brownian dynamics simulations of interacting rod suspensions. For this purpose, we study the behavior of rodlike suspensions under a cross field configuration of shear and electric fields as a function of both the magnitudes of the respective fields and the orientation between them.

The rest of this article is arranged as follows: In the next section we present a simple deterministic analysis of the dynamics of a single rod in an oriented field configuration. We use the latter analysis to suggest that a cross-field shear and electric field configuration may result in a "rotating" state of the rods which may potentially disperse the nanotube suspension. In the section that follows, we present a Smoluchowski equation based analysis of the dynamics of the rod suspensions under combined electric and shear field configuration. Subsequently, we discuss the results of the Brownian dynamics simulation method used to analyze the dynamics of a rodlike suspension in a cross-field configuration.

 Published on Web 08/21/2009

The results of our simulations are in good agreement with the predictions of our analytical theory. We conclude with a few comments on the discrepancies between experiments and theory.

Deterministic Dynamics of a Single Rod under Shear and Electric Fields

In this section, we consider the deterministic dynamics of a single rod under the combined influence of externally imposed shear and electric fields. We first consider independently the effects of shear and electric fields and show that for long rods the preferred state in each of these cases is one where the rod is aligned with the external field. Subsequently, we consider the case where shear and electric fields are imposed simultaneously at an orientation to each other.

Dynamics of a Single Rod under Shear Fields. The deterministic dynamics of nonspherical particles in the presence shear flow fields has been studied extensively.[15] An ellipsoidal particle whose orientation is denoted $\hat{\mathbf{u}}$ rotates in a periodic motion termed as Jeffery orbits with an angular velocity $d\hat{\mathbf{u}}/dt$ governed by:[15]

$$\frac{d\hat{\mathbf{u}}}{dt} = \hat{\mathbf{u}}\cdot\omega + \left(\frac{p^2-1}{p^2+1}\right)(\hat{\mathbf{u}}\cdot\mathbf{D} - \hat{\mathbf{u}}\hat{\mathbf{u}}\hat{\mathbf{u}}\hat{\mathbf{u}}:\mathbf{D}) \tag{2}$$

where $\mathbf{D} \equiv (\nabla\mathbf{v} + (\nabla\mathbf{v})^T)/2$ represents the rate of strain tensor, and $\omega = (\nabla\mathbf{v} - (\nabla\mathbf{v})^T)/2$ represents the vorticity tensor. For spherocylindrical objects, $p \simeq 0.7L/d$, where L and d denote the length and diameter of the object respectively. In a simple shear, the period of rotation of the object P can be deduced as

$$P = \frac{\pi}{\dot{\gamma}}\left(p + \frac{1}{p}\right) \tag{3}$$

where $\dot{\gamma}$ denotes the shear rate. It can be seen that, for $p \to \infty$ (corresponding to an infinitesimally thin rod), $P \to \infty$, representing the fact that a very thin long rod remains practically aligned in the direction of the shear velocity. Hence, it is evident that the use of shear fields alone does not prove efficient in dispersing the aggregated nanotubes.

The above expectation is consistent with many experiments which have considered the effect of shear flows upon the nanotube suspensions. Explicitly, alignment of the nanotubes in the shear direction has been reported in many earlier researches.[13,16−18] Lin-Gibson et al.[5] additionally reported large scale flow instabilities and vorticity-alignment of polymer nanotube composites upon application of shear. They attributed such effects to the viscoelastic properties of the underlying polymer matrix. Flow-induced alignment and concomitant property modifications were also reported in Kharchenko et al.[19]

Contrary to the above results, a few experiments have also reported the dispersion of nanotubes using strong mechanical mixing.[20] While the latter may seem to contradict the above discussion, it may be argued that such mechanical mixing does not correspond to a simple shear field, but rather a more complex flow field which includes extensional components which may aid in breaking the nanotube bundles. A main disadvantage of such a process is the potential degradation of the polymer matrix (and the properties) during the strong fields employed. The strategy explored in this article may be viewed as being complementary to such experimental strategies, where the application of electric fields in a cross-field configuration (under conditions discussed in the following sections) may be used as means to substantially reduce the intensity of flow mixing used in such processes.

Dynamics of Particles in AC Electric and Magnetic Fields. The theory of the dynamics of an anisotropic particle in an AC electric field has been studied in Schwarz et al.[21] If the AC electric field $\mathbf{E}(t)$ represented as

$$\mathbf{E}(t) = \mathbf{E}\cos(\omega_E t + \phi_E) \tag{4}$$

is oscillating with a frequency ω_E much larger than any other relevant frequency in the system, such oscillations can be averaged out and the torque acting on a long rod placed in an AC electric field can be obtained as:[22]

$$\mathbf{T} = \alpha(\hat{\mathbf{u}}\cdot\mathbf{E})\mathbf{E}\times\hat{\mathbf{u}} \tag{5}$$

where the frequency (ω_E) dependent polarizability of the rod in the medium $\alpha(\omega_E)$ is given as[22]

$$\alpha(\omega_E) \propto Ld^2\varepsilon_m\,\mathrm{Re}\left[\frac{\tilde{\varepsilon}_r - \tilde{\varepsilon}_m}{\tilde{\varepsilon}_m}\right] \tag{6}$$

with $\tilde{\varepsilon}_m(\omega_E)$ and $\tilde{\varepsilon}_r(\omega_E)$ denoting the complex dielectric constants of the solvent and the rod respectively, and $\varepsilon_m(\omega_E)$ represents the real component of dielectric constant of the solvent. One can see that the torque is zero if the field is either parallel or perpendicular to the rod. The stable orientation depends on the sign of polarizability α, which can itself be positive or negative (and frequency dependent) depending on the sign of $\mathrm{Re}[\tilde{\varepsilon}_r - \tilde{\varepsilon}_m)/\tilde{\varepsilon}_m]$. For this study, we will assume without loss of generality that $\alpha > 0$, a situation for which the rods align parallel to the direction of the externally applied electric field.

The above suggests that use of electric fields alone only serves to align the rods (nanotubes) in a given direction, and may not help in dispersing the nanotubes. A few experiments which have examined the effects of electric (and magnetic) fields upon nanotube suspensions have indeed come to the same conclusion. Camponeschi et al.[23] demonstrated the magnetic field induced alignment and concomitant property modifications of polymer-nanotubes composites. Koerner et al.[24] demonstrated similar effects using uniaxial magnetic fields. Vaia and co-workers,[25,26] Park et al.,[27] and Zhu et al.[28] report similar alignment effects in the context of external electric fields.

Dynamics of a Single Rod under Combined Shear and Electric (Magnetic) Fields. In this section, we consider the deterministic dynamics of rods resulting from the combined action of shear and electric or magnetic fields. For the case of very long rods and when the velocity field $\mathbf{v}(r) = \kappa\cdot\mathbf{r} + \mathbf{v}_0$, eq 2 governing the dynamics of the rod in linear flow fields may be reduced to:

$$\frac{d\hat{\mathbf{u}}}{dt} = \hat{\mathbf{u}}\times(\kappa\cdot\hat{\mathbf{u}}) \tag{7}$$

Combining the above equation with eq 5, one can obtain the deterministic equation of motion for the rods (in the limit of long rods and averaged AC fields) in the combined presence of an external flow and electric field as

$$\frac{d\hat{\mathbf{u}}}{dt} = \frac{\mathbf{T}}{\xi_r} + \hat{\mathbf{u}}\times(\kappa\cdot\hat{\mathbf{u}}) \tag{8}$$

where $\mathbf{T}$ is given by eq 5 and ξ_r denotes the rotational friction coefficient for the rod. The latter is related to the rotational diffusion coefficient of the rod D_{r0} through $\xi_r \equiv k_B T/D_{r0}$.[29]

To discuss the dynamics of the rods resulting from the above equation of motion, we consider a simple shear flow in the X direction with the vorticity direction denoted by Z for which

$$\kappa = \begin{pmatrix} 0 & \dot{\gamma} & 0 \\ 0 & 0 & 0 \\ 0 & 0 & 0 \end{pmatrix} \tag{9}$$

Further, we assume that $\mathbf{E}$ is located in the $X-Y$ plane at an angle β to the X axis:

$$\mathbf{E} = \begin{pmatrix} \cos\beta \\ \sin\beta \\ 0 \end{pmatrix} \tag{10}$$

Equation 8 can then be solved analytically to obtain the angular velocity of rotation of a rod located in XY plane

$$\omega_z(\phi) = \frac{\dot{\gamma}}{2}\left[\cos 2\phi + \frac{\alpha E^2 D_{r0}}{\dot{\gamma}} \sin(2\beta - 2\phi) - 1\right] \tag{11}$$

where ϕ is the angle between rod and X-axis.

In the event $\omega_z = 0$ for some $\phi = \phi_0$ (and $d\omega_z/d\phi < 0$), we have a state which the rod is aligned at an angle ϕ_0. More interestingly, a state $\omega_z < 0$ for all ϕ is possible if

$$\frac{Pe}{\Xi}|\sin(2\beta)| > \frac{1}{2} \tag{12}$$

where $\Xi = \alpha E^2$ and the Peclet number $\mathrm{Pe} = \dot{\gamma}/D_{r0}$. In such a case, the combined actions of shear and electric fields lead to a continuous rotation of the rods with a nonzero average angular velocity:

$$\langle\omega_z\rangle = \frac{\dot{\gamma}\sqrt{(\Xi/Pe)[2\sin(-2\beta) - (\Xi/Pe)]}}{2} \tag{13}$$

In Figure 1, we depict the above parametric regime wherein combined action of shear and electric fields may lead to a state where the rod continuously rotates without alignment. It can be seen from eqs 12 and 13 that for specified magnitudes of electric and shear fields, an orientation $\beta = -\pi/4$ between the fields offers both the maximum parametric window for achieving a rotating state as well as the maximum average rotation speeds in such states. Alternatively, for a specified orientation between the flow and electric fields (angle β) and shear rate ($\dot{\gamma}$), the maximum average rotation speeds can be seen to be achieved for electric fields such that

$$\frac{Pe}{\Xi}|\sin(2\beta)| = 1 \tag{14}$$

It is also interesting to note that a configuration where $\beta = \pi/2$ (electric and shear fields perpendicular to each other) is the *least conducive* to lead to a rotating state of the rods.

Implications for Dispersing Aggregated Rods Suspensions: A Hypothesis. We now comment on the results of the preceding section and their potential implications in the context of dispersing an an aggregated solution of rods using nonequilibrium fields. Our above deterministic analysis points to the possibility that the use of combined shear and electric fields (at an orientation to each other) may lead to a continuously rotating motion of the rod. While the above analysis pertained to the dynamics of a single rod, to quantify the effects of such an occurrence upon the dispersion state of a suspension, we need to extend the above analysis to address the cooperative dynamics of rod suspensions characterized by strong attractive interactions.

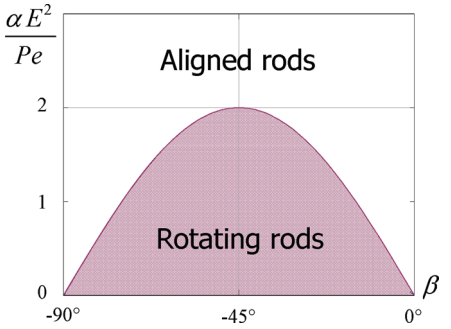

Figure 1. Parametric regime depicting the rotating and aligned states of the rod in combined shear and electric fields.

In the context of an aggregating suspension of rods, the state of the system is not expected to be a homogeneously oriented suspension, but rather is expected to consist of aggregated clusters of rods, each of which is oriented on an average in the direction of macroscopic global alignment. Moreover, the aggregates are expected to be polydisperse in both the aspect ratio and the aggregation numbers. Unfortunately, it is extremely cumbersome to model the combined action of shear and electric fields upon the overall state of such a suspension (in effect, this requires the analysis of a six dimensional variant of the three-dimensional Smoluchowski equation presented in the next section). In this article, we undertake a simpler analysis by studying the combined effects of electric and shear fields upon *homogeneous* rod suspensions. Our premise is that the results of such a model may be used to obtain physical understanding of the orientational dynamics inside a single aggregate (intra-aggregate behavior) in an aggregated suspension of rods. In the next section, we use a combination of theoretical analyses to discern that in a homogeneous solution of rods, the above-deduced rotating state may manifest either as: (i) A cooperative, periodic rotation of the rods which maintains their degree of ordering; or as (ii) An incommensurate rotation of the rods which periodically orders and disorders the suspension. We speculate that the former scenario will maintain the structure of the aggregates and rotate the cluster as a whole. In contrast, we hypothesize that the latter situation would be conducive to compromising the integrity of the aggregates and hence promote dispersion of the aggregated suspension. With this premise we set out to map the parametric regions where a combination of fields leads specifically to a periodic rotation of the orientational directions with intermittent disordering or pulsation of the orientational order. Admittedly, at this stage, our proposal is just a speculative hypothesis. In a subsequent section, we present the results of Brownian dynamics simulations of aggregating rod suspensions and effect a comparison between our theoretical predictions and hypothesis.

Stochastic Dynamics of a Rod Suspension Under Shear and Electric Fields

In this section consider the dynamics of homogeneous suspension of rods. A model for such a system was suggested by Doi and Edwards and has been extensively analyzed under equilibrium and flow conditions.[29,30] In this work, we consider just the orientational state of a suspension of rods (and not the dynamics

of phase separation itself, which requires a much more involved treatment[31−34]) under the combined action of shear and electric fields. The model we use is Doi's self-consistent Smoluchowski equation for the rod orientation distribution function $\Psi(\hat{\mathbf{u}},t)$ function.[29,30] For our situation of combined electric and shear fields, the equation governing $\Psi(\hat{\mathbf{u}},t)$ can be written as:

$$\frac{d\Psi}{dt} = D_r\mathscr{R}\cdot\{\Psi\cdot[\mathscr{R}(\log\Psi+V(\hat{\mathbf{u}}))]-(\hat{\mathbf{u}}\times\kappa\cdot\hat{\mathbf{u}}\Psi)\} \quad (15)$$

where

$$\mathscr{R} = \hat{\mathbf{u}}\times\frac{\partial}{\partial\hat{\mathbf{u}}} \quad (16)$$

denotes the rotational diffusion operator. $V(\hat{\mathbf{u}})$ represents the potential field experienced by the rod and includes both the rod−rod interactions and the effect of the external electric field:

$$V(\hat{\mathbf{u}}) = V_{\text{int}}(\hat{\mathbf{u}})+V_{EF}(\hat{\mathbf{u}}) \quad (17)$$

The rod−rod interactions are usually approximated in a mean-field self-consistent framework as an energy penalizing orientationally disordered states.[29] In such a framework, V_{int} is quantified by a strength U and writtenas:

$$V_{\text{int}}(\hat{\mathbf{u}}) = -\frac{2U}{3}\hat{\mathbf{S}}:\hat{\mathbf{S}} \quad (18)$$

where

$$\hat{\mathbf{S}} = \frac{3}{2}\left(\hat{\mathbf{u}}\hat{\mathbf{u}}-\frac{1}{3}\mathbf{I}\right)$$

quantifies the orientational state of the system, and

$$\mathbf{S} = \int \hat{S}\,\Psi(\hat{\mathbf{u}})\,d\hat{\mathbf{u}}$$

represents the average orientational order parameter. The electric field contribution can be written as a quadrupolar interaction between the field and the orientation:

$$V_{EF}(\hat{\mathbf{u}}) = \frac{2\alpha}{3}\hat{\mathbf{S}}:\hat{\mathbf{E}}\hat{\mathbf{E}} \quad (19)$$

The rotational diffusion coefficient D_r appearing in eq 15 is in principle dependent on both the local concentration of the rods as well as the angular distribution function $\Psi(\hat{\mathbf{u}},\mathbf{t})$.[30] However, we work within the simplifying assumption that D_r depends only upon the average concentration of the rods and treat it as a constant parameter in our calculations below.

Decoupling Approximation. While a numerical solution of the eq 15 is possible using an expansion of $\Psi(\hat{\mathbf{u}},\mathbf{t})$ in spherical harmonics,[35] such a solution proves cumbersome and is not explored here. Instead, we consider a simplification termed the "decoupling approximation" which allows us to solve for the dynamics of the components of the tensorial order parameter $\mathbf{S}$.[33,36] The first step in obtaining such an equation is to multiply both sides of eq 15 by $\hat{\mathbf{S}}$ and integrate over the variable $\hat{\mathbf{u}}$. This leads to:[29,36]

$$\begin{aligned}\frac{dS_{\alpha\beta}}{dt} &= -6D_r[S_{\alpha\beta}+2D_r(2S_{\alpha\mu}+\delta_{\alpha\beta})(US_{\mu\beta}+2\alpha E_\mu E_\beta)\\ &+(US_{\mu\nu}+2\alpha E_\mu E_\nu)\langle\hat{u}_\alpha\hat{u}_\beta\hat{u}_\mu\hat{u}_\nu\rangle]+\frac{(\kappa_{\alpha\beta}+\kappa_{\beta\alpha})}{2}\\ &+(\kappa_{\alpha\mu}S_{\mu\beta}+\kappa_{\beta\mu}S_{\mu\alpha})-3\kappa_{\mu\nu}\langle\hat{u}_\alpha\hat{u}_\beta\hat{u}_\mu\hat{u}_\nu\rangle \end{aligned} \quad (20)$$

where $S_{\alpha\beta}$ denotes the components of the $\mathbf{S}$ tensor, and $\langle\cdots\rangle$ stands for

$$\langle\cdots\rangle = \int(\cdots)\Psi(\hat{\mathbf{u}})\,d\hat{\mathbf{u}}$$

If we assume that that the field $\mathbf{E}$ is defined by eq 10, and $\Psi(\hat{\mathbf{u}})$ is symmetric to orientational reflections about the Z-axis, we can deduce that $\mathbf{S}$ is of the form:

$$\mathbf{S} = \begin{pmatrix} S_{xx} & S_{xy} & 0\\ S_{xy} & S_{yy} & 0\\ 0 & 0 & -S_{xx}-S_{yy}\end{pmatrix} \quad (21)$$

To render eq 20 solvable, one needs an approximation to treat the fourth order moments appearing therein. Decoupling approximations express the fourth order moments in terms of the second order moment (in this case, $\mathbf{S}$),which allows one to derive a closed form equation for the order parameter $\mathbf{S}$. A variety of decoupling approximations have been explored in the literature with different degrees of success for different problems.[37] To treat the fourth order moment accompanying the shear flow term, we use the HL1Q closure,[37] which was shown to be most accurate among the different decoupling approximations for treating the dynamics of rod suspensions in shear flows. Explicitly, in this framework,

$$\begin{aligned}\kappa\cdot\langle\hat{\mathbf{u}}\hat{\mathbf{u}}\hat{\mathbf{u}}\hat{\mathbf{u}}\rangle \simeq \frac{1}{5}[6\langle\hat{\mathbf{u}}\hat{\mathbf{u}}\rangle\cdot\kappa\cdot\langle\hat{\mathbf{u}}\hat{\mathbf{u}}\rangle-(\kappa\\ :\langle\hat{\mathbf{u}}\hat{\mathbf{u}}\rangle)\langle\hat{\mathbf{u}}\hat{\mathbf{u}}\rangle+2((\langle\hat{\mathbf{u}}\hat{\mathbf{u}}\rangle-\langle\hat{\mathbf{u}}\hat{\mathbf{u}}\rangle\langle\hat{\mathbf{u}}\hat{\mathbf{u}}\rangle):\kappa)\mathbf{I}]\end{aligned} \quad (22)$$

To treat the fourth order moments arising in the potential energy terms, we use the commonly employed Gaussian decoupling:[29,36]

$$(US_{\mu\nu}+2\alpha E_\mu E_\nu)\langle\hat{u}_\alpha\hat{u}_\beta\hat{u}_\mu\hat{u}_\nu\rangle \simeq (US_{\mu\nu}+2\alpha E_\mu E_\nu)\langle\hat{u}_\mu\hat{u}_\nu\rangle\langle\hat{u}_\alpha\hat{u}_\beta\rangle \quad (23)$$

Using $\langle\hat{\mathbf{u}}\hat{\mathbf{u}}\rangle = (2\mathbf{S}+\mathbf{I})/3$, the above equations can be recast in terms of $\mathbf{S}$.

The component equations resulting from using the decoupling approximation above are straightforward to derive but cumbersome to list and hence are not displayed here. In this approximation, the model is a function of four parameters: Peclet number, $\text{Pe} = \dot{\gamma}/D_r$, strength of the electric field nondimensionalized as $X = \alpha E^2/\text{Pe}$, the orientation between the field and the direction of the shear velocity β, and the strength of the interaction potential U. We nondimensionalized the time t as $\tau = D_r t$ and numerically integrated the resulting equations for different values of the parameters Pe, Ξ, β, and U. Using the components of the orientational order parameter, the eigenvalues of the $\mathbf{S}$ matrix can be determined. The magnitude of the largest eigenvalue of $\mathbf{S}$ (which we denote as S_2) quantifies the degree of orientational ordering in the system and the direction of the eigenvector corresponding to S_2 constitutes the direction of alignment of the rods (commonly referred to as the direction of the director).

Figure 2 displays a few representative solutions arising from the solution of our decoupling model for the case when $\beta = -\pi/4$. Figure 2a illustrates the effects of combined application of shear and electric fields on a state where the strength of the orientational interactions $U = 0$. We note that the equilibrium solution (in the absence of any external field)

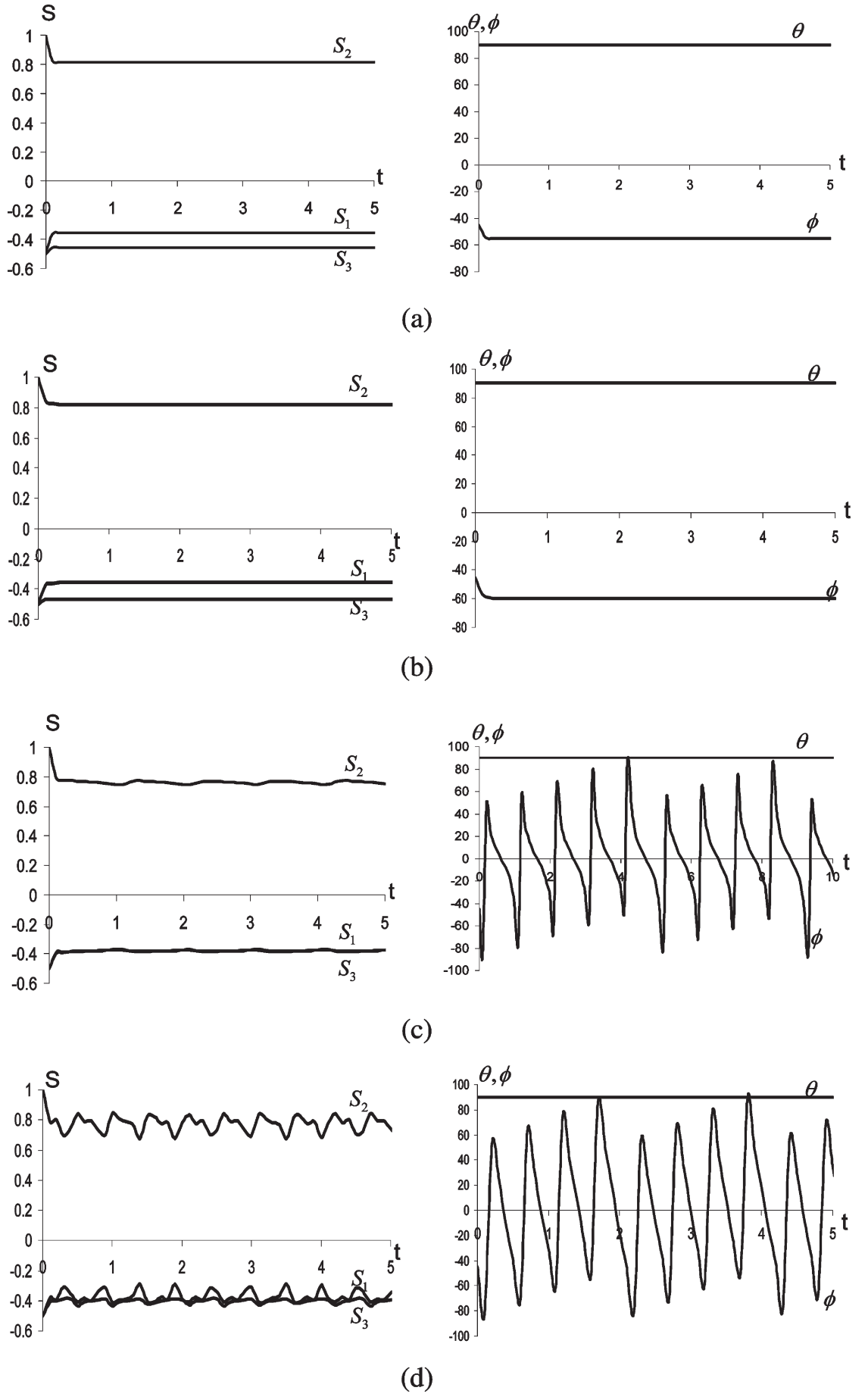

Figure 2. Time evolution of eigenvalues S_1, S_2, and S_3 and the direction θ (angle with respect Z axis) and ϕ (angle with respect to X axis) of the eigenvector corresponding to S_1 of the tensorial order parameter S: (a) $U = 0$, $X = 1$, Pe = 1; (b) $U = 5$, $X = 0.91$, Pe = 1; (c) $U = 5$, $X = 0.0$, Pe = 1; (d) $U = 5$, $X = 0.1$, Pe = 1.

in this case corresponds to a disordered state with $S_2 = 0$. It is seen that applying a shear and an external field results in an orientationally aligned state with the director oriented in the XY plane (represented through the Euler angels θ and ϕ for the director orientation). Figure 2b displays a similar aligned state resulting when $U \neq 0$ and under the combinedaction of the shear and electric fields. Figure 2c displays a solution with stronger orientational interactions which leads to an orientationally ordered state with $S_2 \neq 0$ (which oscillates with very small amplitude), but the direction of alignment (still confined in the XY plane, since $\theta = \pi/2$) oscillates periodically in time. This corresponds to a regime where the rods maintain their degree of alignment but exhibit periodic cooperative rotation. Finally, Figure 2d displays a state where the order parameter is seen to oscillate along with the orientation of the director. The latter corresponds to a regime where the rods exhibit a time periodic partial cooperative rotation (which leads to their partial disordering).

Several earlier studies in the context of simple shear flows have studied the regimes of behavior discussed above and have cataloged the above behaviors into different regimes termed as tumbling, kayaking, wagging etc.[35,38−40] Other studies have also focused on the shift of the phase separation spinodals under the influence of shear flows.[31−33,38] In this study however, we do not embark on a detailed parametric study to delineate the above regimes. Rather, we focus on issues pertinent to rod solutions characterized by strong attractive interactions for which the system is not expected to be an oriented homogeneous suspension. As proposed in the preceding section, we hypothesize that regimes for which aggregates of rods would both rotate periodically and partially disorder are likely to break the aggregates. To delineate the parametric regime which leads to such a state, we consider a measure δS which quantifies the fluctuation of the order parameter S_2 within a period of oscillation of the director. In parts a and b of Figure 3, we display δS as a function as a function of the Peclet number and the parameter X (for $\beta = -\pi/4$). It is seen that at small electric fields (relative to Peclet number), the intensity of fluctuations of the order parameter are negligible. However, upon increasing the parameter X it is observed that the fluctuations in order parameter increase up to $X \simeq 1$ and then decreases thereafter.

The above behavior is reminiscent of the predictions derived in the preceding section using our deterministic model. Indeed, in such a context, we identified that for a specified orientation between the flow and electric fields (angle β) and shear rate ($\dot{\gamma}$), the maximum average rotation speeds can be seen to be achieved for electric fields such that $\mathrm{Pe}/\Xi|\sin(2\beta)| \equiv X^{-1}|\sin(2\beta)|$ (cf. eq 14). The above results confirm that such expectations hold, albeit, with a Pe number dependent behavior which reflects the collective dynamics of the rods.

To use the above results to identify a target regime for the dispersion of rods using electric and shear fields, we need to identify the parameters (β, Pe, and Ξ) where the order parameter fluctuations δS are relevant. Unfortunately, the above decoupling approximation numerically fails at higher (and experimentally more pertinent) Peclet numbers. Shown in Figure 4 is one such case where we can see that a numerical integration of the evolution eqs 20 leads to order parameters which are above a magnitude 1.0, which are clearly inadmissible. However, it is evident from the results of the decoupling approximation that at high enough Peclet numbers (albeit, still within the regime where the decoupling approximation yields physically correct results), the director of the rods are aligned in the XY plane (the director angle

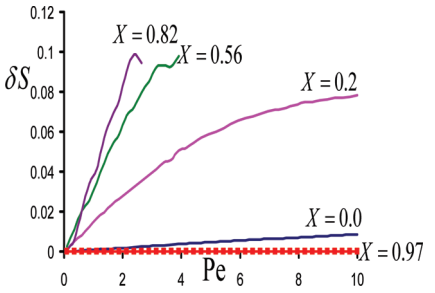

Figure 3. Amplitude of fluctuations of the order parameter for $U = 5$, $\beta = -\pi/4$ as a function of the Peclet number for different X parameters (the values corresponding to $X = 0.97$ are small and hence are represented by symbols). The decoupling approximation and the numerical scheme fails for some Xs at higher Peclet numbers and such a behavior is reflected in the results depicted.

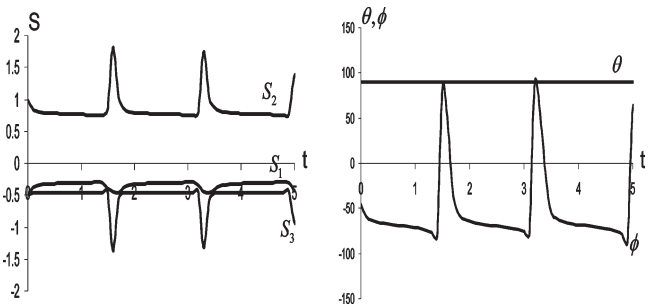

Figure 4. Time evolution of eigenvalues S_1, S_2, and S_3 and the direction θ (angle with respect Z axis) and ϕ (angle with respect to the X axis) of the eigenvector corresponding to S_1 of the tensorial order parameter **S** for $U = 5$, $X = 0.81$, Pe = 1.

$\theta = \pi/2$). This allows us to make such an assumption at the outset and use a two-dimensional (2D) model which can be solved without invoking the decoupling approximation by using an expansion in Fourier coefficients.

2D Model. In two dimensions, we look for a solution of Smoluchowski equation for the 2D angular distribution function $f(\phi,t)$.[41,42] This satisfies

$$\begin{aligned} D_r^{-1}\frac{\partial f}{\partial t} = \frac{\partial^2 f}{\partial \phi^2} + + \frac{1}{2}(\mathrm{Pe} - (\mathrm{Pe} + 4U\langle \sin 2\phi\rangle \\ + \Xi \sin(2\beta))\cos(2\phi) + (4U\langle \cos 2\phi\rangle \\ + \Xi \cos(2\beta))\sin(2\phi))\frac{\partial f}{\partial \phi} + + ((4U\langle \cos 2\phi\rangle \\ + \Xi\cos(2\beta))\cos(2\phi) + (\mathrm{Pe} + 4U\langle \sin 2\phi\rangle \\ + \Xi \sin(2\beta))\sin(2\phi))f(t,\phi) \end{aligned} \quad (24)$$

Such an equation can be solved numerically using a Fourier expansion for $f(t,\phi)$:[42]

$$f(t,\phi) = \frac{1}{2\pi} + \sum_{n=1}^{\infty}(a_n(t)\sin(2n\phi) + b_n(t)\cos(2n\phi)) \quad (25)$$

where $a_n(t)$ and $b_n(t)$ are the Fourier coefficients quantifying the temporal dynamics of $f(\phi,t)$. The Fourier expansion 25 can be substituted into eq 24 to derive evolution equations for the coefficients $a_n(t)$ and $b_n(t)$. To maintain brevity, we eschew the algebraic details here and present just the results arising from the solution of the dynamical equations.

Figure 5 displays the results for the intensity of order parameter oscillations δS as a function Peclet number and the parameter X ($\beta = -\pi/4$, $U = 5$). The behavior of

the variations of δS appears qualitatively similar to the results arising from the decoupling approximation (Figure 3) and our results from the deterministic analysis. Specifically, we see that over a range of the parameter X there manifests a marked increase in the fluctuations in the order parameter δS, corresponding to the regime we speculate to be optimal for dispersion of aggregated rod solutions. For larger X, we observe that δS again becomes negligible, suggesting that the parameters corresponding to this regime may not be optimal for the dispersion of aggregated suspensions.

The above results may be summarized in a "phase diagram" (displayed in Figure 6, parts a and b) which delineates the region where $\delta S \geq 0.01$ (an arbitrary measure of the importance of the fluctuations). It is seen that for a specified orientation β between the fields, there exists a range of parameters quantified by X in which a homogeneous suspension of rods undergoes a motion involving a cooperative rotation of the rods concomitant with a partial disordering. Moreover, it demonstrates that an orientation $\beta = -\pi/4$ between the fields provides a maximal parametric window for achieving such a state over the widest choice of parameters. We note that these results are consistent with the conclusions derived from the analysis of the deterministic motion of a single rod.

Brownian Dynamics Simulations

In the preceding sections, using both the deterministic dynamics of a single rod and the stochastic dynamics of a rod suspension in a combined setup involving shear and electric fields, we presented a speculative hypothesis regarding possible parametric conditions which may promote the dispersion of an aggregated state of nanotubes. In this section, we present Brownian dynamics simulations which examine the validity of the hypothesis and its shortcomings. Explicitly, we considered semidilute rod suspensions characterized by attractive interactions, and examined using Brownian dynamics simulations the combined effects of shear and electric fields upon the aggregation state of the system.[43−45] The simulation methodology used in this article shares similarities to that employed in an earlier article of ours. Consequently, we relegate the discussion of the simulation details and the numerical parameters to the Appendix.[45]

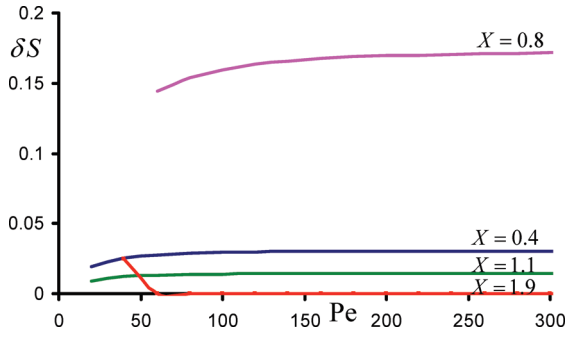

Figure 5. Amplitude of fluctuations of the order parameter for $U = 5$, $\beta = -\pi/4$ as a function of the Peclet number for different X parameters.

Physical Parameters Probed and Nonequilibrium Issues. Our simulations started with a homogeneous dispersed phase which we simultaneously quench in attractive interactions and apply the external shear and electric fields. We probed two values for the electric field, $E = 1$ and $E = 10$, and three shear rates $\gamma = 0.01$, $\dot{\gamma} = 0.001$ and $\dot{\gamma} = 0.0001$. We used the following different angles β between field and the flow: $\beta = 0°$; $-15°$; $-30°$; $-45°$; $-60°$; $\pm 90°$. We considered two cases for the strength of the rod−rod attractions (in k_BT units): (i) $\varepsilon_{bb} = 5$, corresponding to a suspension which upon quench led to finite sized aggregates; (ii) $\varepsilon_{bb} = 11$, corresponding to an unstable suspension in which an equilibrium quench results in a slow, continuous evolution of aggregates.

Before we present the results obtained for the cases studied, we briefly discuss some of the issues encountered in our simulations. Simulations of rod suspensions are by themselves hindered by the extremely slow relaxation times accompanying semidilute and concentrated rod suspensions. Additional time scales arising from aggregation and spinodal decomposition processes also slow the dynamics of rod suspensions characterized by strong attractive interactions. Moreover, finite size effects arising from the interactions between periodic cells may result in frozen, jammed metastable states. As a result, our simulations probing the influence of external fields (shear and/or electric fields) were sometimes plagued by nonergodic frozen states for small magnitudes of shear or electric fields. In the discussion of our results below, we have excluded the situations which led to such frozen states and focused only on parameters for which there was dynamical evolution of the aggregates.

Simulation Results. In Figure 7, we present representative results for $\varepsilon_{bb} = 11$ illustrating the idea proposed in this article. Explicitly, Figure 7a displays the structure in the presence of a weak orientation field and no shear, where extremely slow orientation and aggregation of rods into percolated fibers oriented in the field direction was observed. A weak orientation field $E = 1$, $\beta = \pi/2$ and strong shear $\dot{\gamma} = 0.01$ causes orientation and macroscopic aggregation of the rods. A strong orientation field $E = 10$ at $\beta = -60$ to the velocity direction and strong shear $\dot{\gamma} = 0.01$ is seen to lead to a

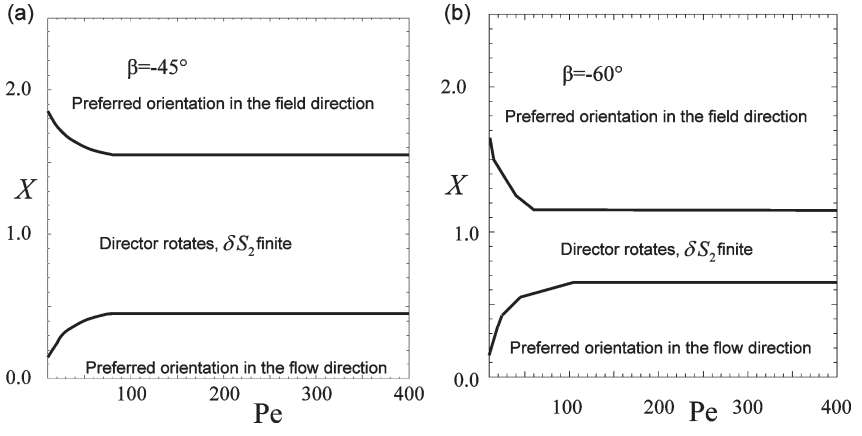

Figure 6. Amplitude of fluctuations of the order parameter for $U = 5$, $\beta = -\pi/4$ as a function of the Peclet number for different X parameters.

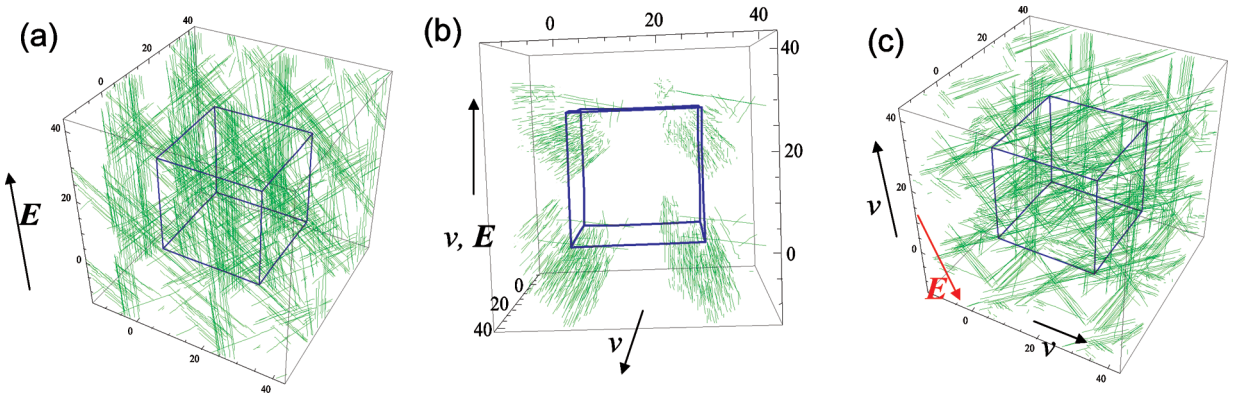

Figure 7. Snapshots of aggregated rod suspensions for: (a) $E = 1, \dot{\gamma} = 0$; (b) $E = 1, \dot{\gamma} = 0.01, \beta = -\pi/2$; (c) $E = 1, \dot{\gamma} = 0.01, \beta = -\pi/3$. The interior box represents the periodic unit cell.

dispersing regime where the fibers become unstable and break to smaller rotating aggregates.

To test a more quantitative comparison to the analytical predictions presented in the preceding sections, we explored a number of different measures to quantify the state of aggregation in our simulations. We note that since the simulations correspond to aggregating rod suspension, direct comparisons with the theoretical predictions of the preceding section (such as the order parameter) is not possible. Instead, we seek to validate our hypothesis that the dispersion state of the simulation system should correlate with the quantity δS deduced in our theory. Quantities such as number of contacts between the rods (defined based on a specified contact distance) were found to be insensitive to the dispersion state of the system. Since the aggregation processes were most clearly reflected in the interrod bead−bead correlation functions $g_{bb}(r)$, we used a measure termed the aggregation number A_{gg} defined as follows:

$$A_{gg} = 4\pi \int_0^\infty (g_{bb}(r) - 1) r^2 \, dr \qquad (26)$$

This can be crudely interpreted as the number of rods in an aggregate. A large value of A_{gg} correlates to an aggregated state whereas a small value of A_{gg} can be correlated to a more dispersed state. Hence, we expect a correlation between ${A_{gg}}^{-1}$ and the parameter δS.

A comparison of our analytical predictions to the simulation results requires knowledge of the rotational diffusion coefficient D_r. In general, D_r is expected to be a function of the concentration of the rod suspension and the strength of the attractive interactions between the rods, but the general functional form for which is unknown. For the purposes of the comparison, we used D_r as a single, free parameter which was chosen to achieve the best correspondence between the simulations and the analytical predictions. Explicitly, for comparisons to the analytical predictions, we used a rotational diffusion coefficient of $D_r = 7.5 \times 10^{-5} s^{-1}$, whereas the actual D_r for the nonaggregated suspension was estimated to be $1.11 \times 10^{-5} s^{-1}$. We comment on this aspect at a later stage.

In Figure 8, we display a comparison of the inverse of aggregation numbers A_{gg} with the δS values computed from our 2D model. In this comparison, the Pe, U, Ξ, and β were kept the same between the simulations and the theoretical model. It is apparent that there is a very good correlation between the regions of large δS and the regions of low aggregation numbers. This confirms our original hypothesis that a combination of shear and electric fields (oriented at an angle) can be used as an effective means to

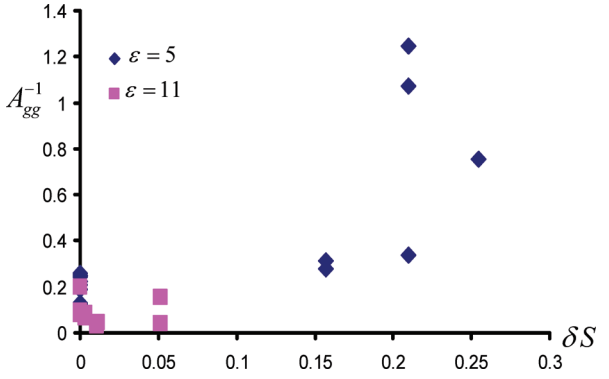

Figure 8. Correlation between aggregation numbers A_{gg} of Brownian dynamics simulations (defined by eq 26 and the fluctuations of the order parameter δS obtained using the 2D Smoluchowski model.

disperse aggregated nanotube suspensions. Moreover, it lends validity to the measure we used (δS) to identify regions and the mechanisms by which optimal dispersion may be achieved.

In comparing our analytical predictions with the results of simulations, it is also evident that there are regions where small δS leads to low aggregation numbers. The latter appears to contradict the fundamental hypothesis underlying the analysis presented in this article. This discrepancy may be a result of the fact that our analytical model concerns the dynamics of a homogeneous suspension of rods. The simulation conditions are far from being homogeneous, and instead correspond to parameters which lead to aggregated, metastable configurations. A better analytical description should consider the dynamics of a two-phase rod solution under the combined action of shear and electric field. For this same reason, use of a single D_r (which enters the Peclet number) to compare the simulations and theory is expected to work only at a qualitative level. Explicitly, the use of a single D_r corresponding to its value for the average solution concentration is expected to be valid only for conditions corresponding to well-dispersed rods (for which the correlation depicted in Figure Figure 8 does improve). However the simulations (and real systems) consists of aggregates of rods which are polydisperse in aspect ratios and hence their diffusivities.

Despite the above cautionary statements which emphasize the qualitative nature of our theory and the reasons for the discrepancies, it is apparent that our theory does a reasonable job of identifying the regions where potentially a combination of electric and shear fields may enhance the dispersion of the nanotubes (as seen in the fact that large δS

does correspond to smaller A_{gg}). Moreover, since many qualitative features unearthed in the context of the deterministic model were found to hold for the stochastic description, the deterministic analysis by itself provides a simple model for exploring the use of a combination of electric and shear fields to promote the dispersion of aggregated nanotube suspension.

Summary

In this article, we proposed a hypothesis that a combination of electric and shear fields at an angle may be used to enhance the dispersion of aggregated rod solution. While our interests were motivated by some of the practical issues facing the dispersion of nanotubes in polymer matrices, our study provides fundamental insights on the dynamics of rod suspensions under the combined action of flow and electric fields. In a nutshell, our analysis and simulation results confirmed our hypothesis and we demonstrated enhanced dispersion of the aggregated rod suspensions for conditions promoting an incommensurately rotating state of the rod suspension. However, to render a more quantitative comparison between the simulations and theory requires one to undertake an analysis of the effects of the field combinations upon the dynamics of phase separation in rod solutions. We propose to study such issues in a future publication.

Acknowledgment. We thank Dr. Richard Vaia for suggesting some of the ideas pursued in this article. We acknowledge financial support from the US Army Research Office under Grant W911NF-07-1-0268, AFOSR's CONTACT program, and the donors of the Petroleum Research Fund, administered by the Americal Chemical Society.

Appendix: Brownian Dynamics Simulation Methodology

In our simulations, the rods are represented as a string of spherical beads linked together in a "shish-kebab" model. Each of these spherical beads interact pairwise by steeply repulsive Lennard-Jones (LJ) potentials truncated at the attractive upturn. The rod is assumed to consist of n_b beads of diameter σ. The overall length of the rod is denoted as L. To track the dynamics of the rod units, we employ an equation of motion for the overall center of mass and orientation of the rods based on the total force and torque experienced by the rods. Explicitly, if we denote the location of the center of mass of the i^{th} rod as $\mathbf{r}^i$ and its orientation as $\hat{\mathbf{u}}^i$, then the position of the j^{th} bead ($j=1...n_b$) on the rod $\mathbf{r}_j^i$ can be obtained as

$$\mathbf{r}_j^i = \mathbf{r}^i + \frac{L(2j-n_b-1)}{2(n_b-1)}\hat{\mathbf{u}}^i = \mathbf{r}^i + \left((j-1)\lambda - \frac{L}{2}\right)\hat{\mathbf{u}}^i \tag{27}$$

where $\lambda = L/n_b - 1$. The bead−bead interaction potential for the rod units $U(r)$ was chosen to be a truncated Lennard-Jones potential:

$$U(r) = \begin{cases} 4\varepsilon_{bb}\left((\sigma/r)^{12} - (\sigma/r)^6 + \frac{1}{2}(\sigma^{12}-\sigma^6)(3r-5)\right) & r<1 \\ 0 & r>1 \end{cases} \tag{28}$$

Here we set $\sigma = 0.65$. The total forces $\mathbf{F}_i$ and the torque $\mathbf{T}_i$ acting on the i^{th} rod can be expressed as the sums of the individual external forces $\mathbf{F}_j^i$ and torques experienced by the bead j as

$$\mathbf{F}_i = \sum_{j=1}^{n_b} \mathbf{F}_j^i \tag{29}$$

$$\mathbf{T}_i = \sum_{j=1}^{n_b}\left(\mathbf{r}^i - \hat{\mathbf{u}}^i\lambda\left(j - \frac{n_b+1}{2}\right)\right) \times (\mathbf{F}_j^i - \mathbf{F}_i) + \alpha(\hat{\mathbf{u}}^i \cdot \mathbf{E})\mathbf{E} \times \hat{\mathbf{u}}^i \tag{30}$$

The second term in the torque above reflects the fact that the presence of an external electric field results in an additional torque (cf. eq 5).

The Brownian dynamics simulations effect a numerical integration of the rotational and translation Langevin equation for the dynamics of the rods acted upon by the above forces and torques. In the following, we set $k_BT = 1$. Explicitly, the rotational dynamics is governed by (subscripts and superscripts are suppressed to maintain brevity):

$$\frac{\mathrm{d}\hat{\mathbf{u}}}{\mathrm{d}t} = \omega \times \hat{\mathbf{u}} \tag{31}$$

where

$$\omega = \frac{T+\eta_r(t)}{\xi_r} + \hat{\mathbf{u}} \times (\boldsymbol{\kappa} \cdot \hat{\mathbf{u}}) \tag{32}$$

in which η_r represents a random noise which satisfies (fluctuation−dissipation theorem)

$$\eta_r(t) = \sqrt{2\xi_r}\varepsilon_r(t) \tag{33}$$

with

$$\langle \varepsilon_r(t) \rangle = 0; \langle \varepsilon_r(t)\varepsilon_r(t') \rangle = \mathbf{I}\boldsymbol{\delta}(t-t') \tag{34}$$

For the rotational friction coefficient, we use the results from Kirkwood theory:[29]

$$\xi_r \simeq \frac{\pi\eta_0 L^3}{3\left(\log\frac{L}{b} - 0.8\right)} \tag{35}$$

The translation dynamics of the center of mass of the rods are governed by

$$\frac{\mathrm{d}\mathbf{r}}{\mathrm{d}t} = \boldsymbol{\kappa} \cdot \mathbf{r} + \frac{1}{\xi_\perp}\mathbf{M} \cdot (\mathbf{F} + \eta_t(t)) \tag{36}$$

where

$$\mathbf{M} = \mathbf{I} + \varkappa\hat{\mathbf{u}}\hat{\mathbf{u}} \tag{37}$$

in which $\varkappa = \xi_\perp - \xi_\parallel)/\xi_\parallel$ where $\xi_\perp$ and $\xi_\parallel$ denote respectively the perpendicular and parallel components of the rod's translational friction coefficient. Within the context of Kirkwood theory for the dynamics of rods[29]

$$\xi_\perp \simeq \frac{4\pi\eta_0 L}{\log\frac{L}{b}}; \xi_\parallel = \frac{\xi_\perp}{2} \tag{38}$$

and hence $\varkappa \simeq 1$. The random noise η_t satisfies

$$\eta_t = \sqrt{2\xi_\perp}\mathbf{C} \cdot \varepsilon_t(t) \tag{39}$$

with

$$\langle \varepsilon_t(t) \rangle = 0; \langle \varepsilon_t(t)\varepsilon_t(t') \rangle = \mathbf{I}\boldsymbol{\delta}(t-t') \tag{40}$$

and

$$\mathbf{C}\cdot\mathbf{C} = \mathbf{M}^{-1} \tag{41}$$

In principle, there is a vast parameter space to be explored for the present study. However, since we were mainly concerned with phenomena resulting from the combined effects of electric and shear fields, we kept many of the geometrical and suspension parameters fixed and studied only the effects of varying the magnitudes of the electric and shear fields and the orientation between them. Explicitly, we fixed the diameter of the bead $\sigma = 0.65$ and $L = 20$ (corresponding to $n_b = 32$ beads). The friction coefficients were fixed such that $\xi_\perp^{-1} = L^{-1} = 0.05$ and $\xi_r^{-1} \equiv 12\xi_\perp^{-1}/L^2 = 0.0015$. Polarizability of the rod was set to $\alpha = 1$. We considered a semidilute to near concentrated suspension with concentration c fixed to $L^3c \approx 128$, $\sigma L^2 c \approx 4.1$. This value of the overall concentration corresponds to a value below the concentration corresponding to isotropic−nematic transition for a solution of rods interacting only through excluded volume interactions.

References and Notes

(1) Baughman, R. H.; Zakhidov, A. A.; de Heer, W. A. *Science* **2002**, *297*, 787–792.
(2) Moniruzzaman, M.; Winey, K. I. *Macromolecules* **2006**, *39*, 5194–5205.
(3) Murakami, H.; Nakashima, N. *J. Nanosci. Nanotechnol.* **2006**, *6*, 16–27.
(4) Krishnamoorti, R.; Vaia, R. A. *J. Polym. Sci., Part B: Polym. Phys.* **2007**, *45*, 3252–3256.
(5) Lin-Gibson, S.; Hobbie, E.; Wang, H.; Pathak, J. *Abstr. Pap. Am. Chem. Soc.* **2003**, *226*, U359.
(6) Szleifer, I.; Yerushalmi-Rozen, R. *Polymer* **2005**, *46*, 7803–7818.
(7) Chatterjee, T.; Krishnamoorti, R. *Phys. Rev. E* **2007**, *75*, 050403.
(8) Warner, M.; Flory, P. J. *J. Chem. Phys.* **1980**, *73*, 6327–6332.
(9) Lekkerkerker, H. N. W.; Coulon, P.; Vanderhaegen, R.; Deblieck, R. *J. Chem. Phys.* **1984**, *80*, 3427–3433.
(10) Surve, M.; Pryamitsyn, V.; Ganesan, V. *Macromolecules* **2007**, *40*, 344–354.
(11) Balasubramanian, K.; Burghard, M. *Small* **2005**, *1*, 180–192.
(12) Delozier, D.; Watson, K.; Smith, J.; Clancy, T.; Connell, J. *Macromolecules* **2006**, *39*, 1731–1739.
(13) Nativ-Roth, E.; Yerushalmi-Rozen, R.; Regev, O. *Small* **2008**, *4*, 1459–1467.
(14) Qu, Y. L.; Chow, W. W. Y.; Ouyang, M. X.; Tung, S. C. H.; Li, W. J.; Han, X. L. *IEEE Trans. Nanotechnol.* **2008**, *7*, 565–572.
(15) Larson, R. *The Structure and Rheology of Complex Fluids*; New York, 1999.
(16) Hobbie, E. K.; Wang, H.; Kim, H.; Lin-Gibson, S.; Grulke, E. A. *Phys. Fluids* **2003**, *15*, 1196–1202.
(17) Camponeschi, E.; Florkowski, B.; Vance, R.; Garrett, G.; Garmestani, H.; Tannenbaum, R. *Langmuir* **2006**, *22*, 1858–1862.
(18) Hobbie, E. K.; Fry, D. J. *J. Chem. Phys.* **2007**, *126*, 124907.
(19) Kharchenko, S.; Douglas, J.; Obrzut, J.; Grulke, E.; Migler, K. *Nat. Mater.* **2004**, *3*, 564–568.
(20) Masuda, J.; Torkelson, J. M. *Macromolecules* **2008**, *41*, 5974–5977.
(21) Schwarz, G.; Saito, M.; Schwan, H. P. *J. Chem. Phys.* **1965**, *43*, 3562–3569.
(22) Morgan, H.; Green, N. G. *AC Electrokinetic: Colloids and Nanoparticles*; Research Studies Press: Baldock, Hertfordshire, U.K., 2003.
(23) Camponeschi, E.; Vance, R.; Al-Haik, M.; Garmestani, H.; Tannenbaum, R. *CARBON* **2007**, *45*, 2037–2046.
(24) Koerner, H.; Hampton, E.; Dean, D.; Turgut, Z.; Drummy, L.; Mirau, P.; Vaia, R. *Chem. Mater.* **2005**, *17*, 1990–1996.
(25) Koerner, H.; Jacobs, D.; Tomlin, D.; Busbee, J.; Vaia, R. *Adv. Mater.* **2004**, *16*, 297.
(26) Lu, W.; Koerner, H.; Vaia, R. *Appl. Phys. Lett.* **2006**, *89*, 223118.
(27) Park, C.; Wilkinson, J.; Banda, S.; Ounaies, Z.; Wise, K. E.; Sauti, G.; Lillehei, P. T.; Harrison, J. S. *J. Polym. Sci., Part B: Polym. Phys.* **2006**, *44*, 1751–1762.
(28) Zhu, Y. F.; Ma, C.; Zhang, W.; Zhang, R. P.; Koratkar, N.; Liang, J. *J. Appl. Phys.* **2009**, *105*, 054319.
(29) Doi, M.; Edwards, S. *The Theory of Polymer Dynamics*; Oxford University Press: Oxford, U.K., 1986.
(30) Doi, M.; Edwards, S. F. *J. Chem. Soc., Faraday Trans. II* **1978**, *74*, 560–570.
(31) Olmsted, P. D.; Goldbart, P. *Phys. Rev. A* **1990**, *41*, 4578–4581.
(32) Olmsted, P. D.; Goldbart, P. M. *Phys. Rev. A* **1992**, *46*, 4966–4993.
(33) Lenstra, T. A. J.; Dogic, Z.; Dhont, J. K. G. *J. Chem. Phys.* **2001**, *114*, 10151–10162.
(34) Tao, Y. G.; den Otter, W. K.; Dhont, J. K. G.; Briels, W. J. *J. Chem. Phys.* **2006**, *124*, 134904.
(35) Larson, R. G. *Macromolecules* **1990**, *23*, 3983–3992.
(36) See, H.; Doi, M.; Larson, R. *J. Chem. Phys.* **1990**, *92*, 792–800.
(37) Feng, J.; Chaubal, C. V.; Leal, L. G. *J. Rheol.* **1998**, *42*, 1095–1119.
(38) Lettinga, M. P.; Dhont, J. K. G. *J. Phys.: Condensed Matter* **2004**, *16*, S3929–S3939.
(39) Tao, Y. G.; den Otter, W. K.; Briels, W. J. *Phys. Rev. Lett.* **2005**, *95*, 237802.
(40) Tao, Y. G.; den Otter, W. K.; Briels, W. J. *J. Chem. Phys.* **2006**, *124*, 204902.
(41) Marrucci, G.; Maffettone, P. L. *Macromolecules* **1989**, *22*, 4076–4082.
(42) Tse, K. L.; Shine, A. D. *J. Rheol.* **1995**, *39*, 1021–1040.
(43) Bitsanis, I.; Davis, H. T.; Tirrell, M. *Macromolecules* **1988**, *21*, 2824–2835.
(44) Yamane, Y.; Kaneda, Y.; Dio, M. *J. Non-Newtonian Fluid Mech.* **1994**, *54*, 405–421.
(45) Pryamitsyn, V.; Ganesan, V. *J. Chem. Phys.* **2008**, *128*, 134901.